

Multimodal Federated Learning with Missing Modality via Prototype Mask and Contrast

Guangyin Bao, Qi Zhang, Duoqian Miao, Zixuan Gong, Liang Hu
Tongji University

{baogy, zhangqi_cs, dqmiao, gongzx, lianghu}@tongji.edu.cn

Abstract

In real-world scenarios, multimodal federated learning often faces the practical challenge of intricate modality missing, which poses constraints on building federated frameworks and significantly degrades model inference accuracy. Existing solutions for addressing missing modalities generally involve developing modality-specific encoders on clients and training modality fusion modules on servers. However, these methods are primarily constrained to specific scenarios with either unimodal clients or complete multimodal clients, struggling to generalize effectively in the intricate modality missing scenarios. In this paper, we introduce a prototype library into the FedAvg-based Federated Learning framework, thereby empowering the framework with the capability to alleviate the global model performance degradation resulting from modality missing during both training and testing. The proposed method utilizes prototypes as masks representing missing modalities to formulate a task-calibrated training loss and a model-agnostic uni-modality inference strategy. In addition, a proximal term based on prototypes is constructed to enhance local training. Experimental results demonstrate the state-of-the-art performance of our approach. Compared to the baselines, our method improved inference accuracy by 3.7% with 50% modality missing during training and by 23.8% during uni-modality inference. Code is available at <https://github.com/BaoGuangYin/PmcmFL>.

1. Introduction

Multimodal pre-trained models have exhibited superior performance in various downstream tasks [4, 33, 35], with the availability of large-scale data being a major contributing factor. However, collecting large-scale data in practical applications may result in privacy leakage. An alternative approach is to adopt a decentralized machine learning paradigm, such as federated learning (FL). In FL [23], distributed clients collaborate to train a global model without

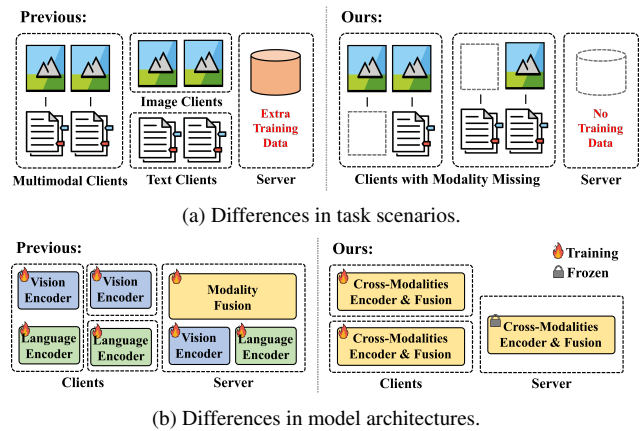


Figure 1. Illustration of differences between our work and previous works [14, 36, 39]. For **task scenarios**, previous works consider two types of clients: unimodal clients and modality-complete multimodal clients. In contrast, our task scenario involves the possibility of partial modalities being missing on each client. In addition, previous works have placed a training set on the server, which is not the case for our solution. For **model architectures**, previous works train modality-specific encoders for each modality and then train the modality fusion module on the server. In contrast, to avoid extra training on the server, we develop local models with the interactive-encoder architecture encompassing modality encoding and fusion.

sharing their private datasets. While FL can provide ample data and efficient communication for training multimodal models, it faces practical challenges when dealing with complex real-world multimodal data. One such challenge is the widely-existing issue of missing modalities. The presence of missing modalities on each client poses constraints on federated architecture while leading to a significant drop in global model inference accuracy. Furthermore, the non-independent and non-identically distributed (non-IID) nature of data among clients [11, 16, 17, 24, 26, 40] sharpens the challenges of modality missing, highlighting the urgent need to address the issue in practical multimodal data.

Some pioneer works [3, 8, 14, 36, 39] attempt to carry out multimodal federated learning with missing modalities.

These approaches employ modality-specific encoders for each modality, such as visual encoders for images and language encoders for text, and train them using unimodal or self-supervised training tasks. Their local encoders are then either aggregated into a global encoder [39], or the global encoder is trained by aligning the local encoders through knowledge distillation (KD) on public data [36]. To perform downstream tasks that require modality fusion, additional training data are necessary to train a modality fusion module on the server. These previous works have primarily focused on specific scenarios of modality missing, either considering unimodal clients or multimodal clients without missing modalities (as shown in Figure 1a). However, in practical scenarios, it is common for each client to have missing data in each modality [8]. A practical example is observed in social media platforms where users commonly generate three types of data: images only, text only, and image-text pairs, leading to a more intricate situation of modality missing.

To address such an intricate situation of modality missing, the existing FL frameworks encounter the following issues (as shown in Figure 1): 1) The dual-encoder architecture [27] cannot obtain deep fused representations in clients due to a lack of cross-modal interaction. 2) Severe task drift occurs between clients and server, e.g., image/text classification on clients but visual question answering (VQA) on the server, resulting in inconsistent optimization directions. 3) Lack of any strategy for addressing inference with missing modalities on the server. 4) The availability of public data and the server’s downstream task datasets has also been controversial in FL. These motivate us to propose a new general multimodal FL framework for real-world modality missing and fused representations learning.

In this paper, we aim to empower the FL framework with the ability to handle the intricate modality missing scenarios during both training and testing. Moreover, we plan to develop models with the interactive-encoder architecture [13] for each client, which can perform both modality embedding and modality interaction. Figure 1b illustrates the distinctions in model architectures between previous works and ours. To this end, we need to address three challenges: CH1) How to handle complex missing patterns for interactive encoder? CH2) How to perform fused representation learning when data is non-IID and modalities are missing? CH3) How do we ensure the performance of the global model when there are missing modalities during inference?

Specifically, we innovatively utilize the flexible Multiway Transformers [1, 25, 33] to construct our multimodal encoders. By selecting different modality expert networks, Multiway Transformers can serve as both modality-specific encoders and interactive encoders, thereby adapting to complex patterns of modality missing (CH1). Inspired by prototype learning in FL [2, 5, 12, 18, 20, 34], we then propose a novel prototype-based multimodal FL framework, termed

PmcmFL (Prototype Mask and Contrast for Multimodal FL) to achieve fused representation learning with non-IID data and missing modalities (CH2). PmcmFL uses prototypes as global prior knowledge of the missing modality to compensate for cross-modal fusion and reduce heterogeneity among clients. Accordingly, we construct and maintain a prototype library, a plug-and-play component for FL. During training, the prototype library incorporates global prior knowledge into local training and calibrates task drift caused by missing modalities. We also construct a proximal item based on the prototype to assist clients in learning fused representations clustered by class. Consequently, we utilize global prior knowledge from the prototype library for inference with missing modalities (CH3), where various matching algorithms are elaborately introduced to identify the prototype with the closest semantics.

Our experiments show that PmcmFL achieves state-of-the-art performance. Notably, it brings 0.2-3.7% accuracy improvements across different modality missing rates. Regarding inference with missing modalities, it achieves a remarkable 23.8% accuracy improvement.

The main contributions are summarized below:

- Our work stands out as the first attempt to empower our FL framework with the capability to alleviate the global model performance degradation resulting from modality missing during both training and testing.
- We propose a novel prototype-based multimodal federated learning framework to achieve task-calibrated training and higher inference accuracy when dealing with modality-incomplete data.
- To the best of our knowledge, we are the first to adopt Multiway Transformer as a versatile encoder to address the complex patterns of modality missing.

2. Related Work

2.1. Multimodal Learning

Multimodal learning has attracted increasing attention from the research community. The model with dual-encoder architecture [27] uses separate encoders for each modality, with shallow modality interaction. On the contrary, the models with interactive-encoder architecture [13, 33] process input from different modalities and concentrate on modeling modality interactions via fuse tokens without modality-specific encoders.

In order to overcome the missing modality issue in multimodal learning, many methods have been developed. Ma et al. [21] propose the SMIL to train a feature reconstruction network using a meta-learning algorithm. Zhao et al. [38] propose the MMIN to learn robust multimodal representations by training cascade residual autoencoders. Ma et al. [22] enhance the robustness of Transformer through multi-task learning and optimal fusion strategy search.

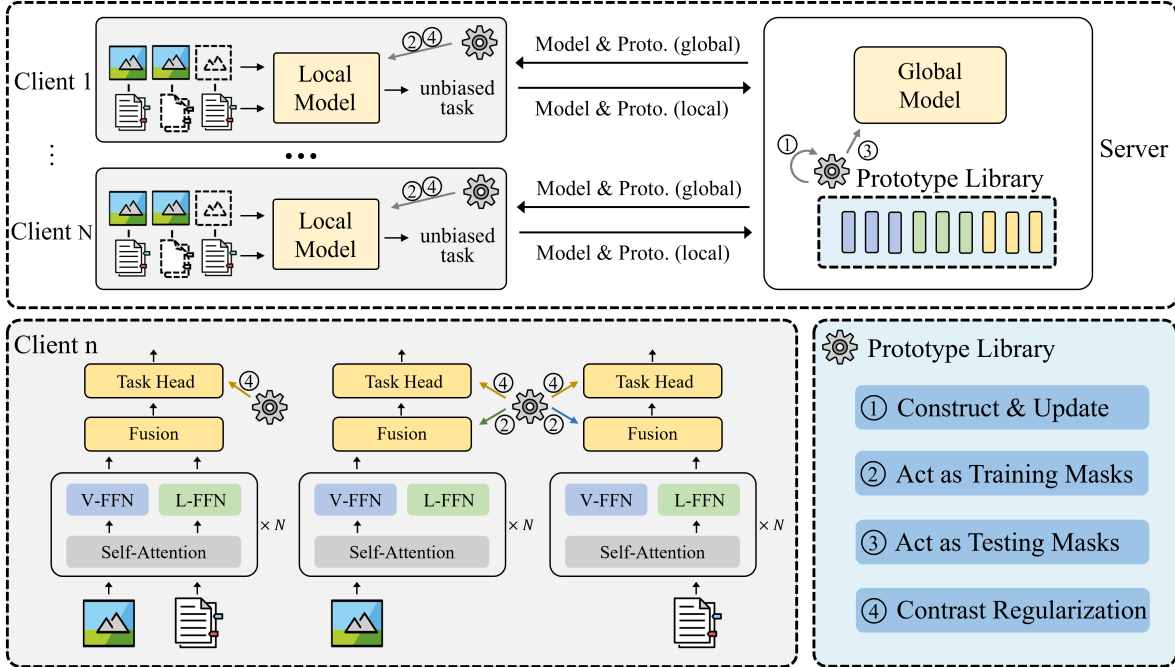


Figure 2. An overview of the proposed PmcmFL. The prototype library is a plug-and-play component in FL. We choose specific representations to construct this prototype library (in Sec.3.2). Based on this, prototypes act as masks to aid training and inference with missing modalities (in Sec.3.3). Besides, we utilize prototypes to construct contrastive loss for better learning of fused representations (in Sec.3.4).

Wang et al. [32] propose the ShaSpec to generate features of missing modalities using a shared encoder. These methods have introduced additional branches and complex training algorithms to the model, which are unsuitable for FL.

2.2. Federated Learning with Prototype

Prototype refers to the centroid of the instances belonging to the identical class [29]. Due to its scalability, prototypes are widely used to solve various problems in FL [15, 18–20]. Tan et al. [30] propose FedProto to conduct FL using prototypes rather than aggregation. Huang et al. [12] utilize prototypes to solve domain shift in FL. Dai et al. [5] utilize prototypes to alleviate the performance decline caused by heterogeneous data in FL. Some other FL frameworks [2, 34], while not explicitly mentioning prototypes, still leverage the concept of prototypes to address corresponding issues. In this paper, we primarily utilize prototypes to address modality missing issues.

2.3. Multimodal Federated Learning

Combining multimodal learning with federated learning is a novel research problem, with the key challenge being how to perform modality interactions when there are missing modalities for each client. Zhao et al. [39] propose FedIoT to train autoencoders for each modality on every client and give more aggregation weight to multimodal clients. Chen et al. [3] propose FedMSplit to construct a dynamic

graph for adaptively selecting multimodal client models where some modalities may be missing. Yu et al. [36] propose CreamFL to conduct cross-modal interaction using inter-modal and intra-modal contrast. However, these studies only considered scenarios involving either unimodal or modality-complete multimodal clients. Feng et al. [8] propose FedMultimodal as the first attempt to consider scenarios where modalities of partial data may be missing on each client. They address this by masking the missing modalities using zero tensors. In this paper, we consider scenarios similar to FedMultimodal, with a focus on an efficient and versatile method for addressing modality missing.

3. Methodology

3.1. Overview

We consider a heterogeneous federated learning setting where N multimodal clients train a global model collaboratively. Without loss of generality, we take images and text as instances of multimodal data. We decouple the model architecture into a representation encoder \mathcal{E} , a deep fusion layer \mathcal{F} , and a task head \mathcal{G} . In each image-text pair, the image or text will be missing with a probability of p . In this case, all the images can be denoted as $\mathcal{I}_n = \{(i_{nk}, y_{nk})\}_{k=1}^{|\mathcal{I}_n|}$, where i_{nk} is the k -th image on the n -th client, y_{nk} is its corresponding label. Similarly, all the text can be denoted as $\mathcal{T}_n = \{(t_{nk}, y_{nk})\}_{k=1}^{|\mathcal{T}_n|}$, and all the image-text pairs

can be denoted as $\mathcal{M}_n = \{(i_{nk}, t_{nk}, y_{nk})\}_{k=1}^{|\mathcal{M}_n|}$. Furthermore, each client develops a local model $(\mathcal{E}_n, \mathcal{F}_n, \mathcal{G}_n)$, $n \in [1 \dots N]$, with the same architecture as the global model.

As shown in Figure 2, PmcmFL constructs/updates the prototype library on the server (operation ①) at the beginning of each federated communication round. Subsequently, the prototype library and the global model are broadcast to all participants. Then, each participating client performs local training and updates local prototypes in parallel. Using prototypes as masks of missing modalities, a task-calibrated training loss will supervise the training (operation ②). Additionally, to tackle the non-IID issue and the resulting client drift, the prototype library introduces a prototype-based contrastive loss to enhance the learning of fused representations (operation ④). Finally, all participating clients transmit their local models and local prototypes back to the server, after which the global model is updated by aggregating those local models. During testing, the prototype library also assists inference with missing modalities by transmitting prototypes to the global model (operation ③). The complete algorithm is in Appendix A.

For local training, the multiway encoder [1, 25, 33] handles different missing patterns by switching among various encoding modes. When only image or text input exists, the multiway encoder functions as a modality-specific encoder, like ViT [7] or BERT [6]. It achieves this by utilizing corresponding modality expert networks (FFN layers). When inputting an image-text pair, the multiway encoder functions as an interactive encoder, enabling the representation of one modality to fuse information from the other modality. It achieves this by utilizing a shared self-attention layer. More discussion on the multiway encoder is in Appendix B.

3.2. Constructing Prototype Library

Prototypes compact the semantics of data within the same class. Considering communication overhead in FL, low-dimensional representations are used to construct the prototype library. As for the compacting strategy, we naively use the class centroids as the prototypes.

Selecting Hidden Representations. For $(i_{nk}, t_{nk}) \in \mathcal{M}_n$, we denote $\mathbb{H}_{nk} = \mathcal{E}_n(i_{nk}, t_{nk}) \in \mathbb{R}^{m \times d}$ as the output of the multiway transformer encoder. Here, m represents the number of output tokens, and d denotes the dimension of each token. The image CLS token $h_{nk}^{(i)}$ and the text CLS token $h_{nk}^{(t)}$ can be extracted from \mathbb{H}_{nk} . We select these two CLS tokens as low-dimensional representations for constructing prototypes. Moreover, the fused representation, denoted as $h_{nk}^{(f)} = \mathcal{F}_n(h_{nk}^{(i)}, h_{nk}^{(t)})$, is also selected for constructing prototypes.

Prototype Library. In the prototype library, we construct and maintain three types of prototypes: image prototypes $\mathcal{P}_{\mathcal{I}}$, text prototypes $\mathcal{P}_{\mathcal{T}}$, and fusion prototypes $\mathcal{P}_{\mathcal{F}}$. All prototypes are initialized with zero tensors or random

tensors from a standard normal distribution. Subsequently, after local training in each federated communication round, all participating clients construct local prototypes by computing class centroids. Finally, the global prototypes are aggregated from the local prototypes with numbers of client samples as weights, the same as FedAvg. The construction process is formalized as follows:

$$\mathcal{P}_{\mathcal{I}_n}^j = \sum_{k \in C_n^j} \frac{h_{nk}^{(i)}}{|C_n^j|}, \quad \mathcal{P}_{\mathcal{I}}^j = \sum_{n \in P_c} \frac{|\mathcal{I}_n|}{|\mathcal{D}|} \mathcal{P}_{\mathcal{I}_n}^j, \quad (1)$$

$$\mathcal{P}_{\mathcal{T}_n}^j = \sum_{k \in C_n^j} \frac{h_{nk}^{(t)}}{|C_n^j|}, \quad \mathcal{P}_{\mathcal{T}}^j = \sum_{n \in P_c} \frac{|\mathcal{T}_n|}{|\mathcal{D}|} \mathcal{P}_{\mathcal{T}_n}^j, \quad (2)$$

$$\mathcal{P}_{\mathcal{F}_n}^j = \sum_{k \in C_n^j} \frac{h_{nk}^{(f)}}{|C_n^j|}, \quad \mathcal{P}_{\mathcal{F}}^j = \sum_{n \in P_c} \frac{|\mathcal{M}_n|}{|\mathcal{D}|} \mathcal{P}_{\mathcal{F}_n}^j, \quad (3)$$

where C_n^j denotes the data of class j on the n -th client, P_c denotes the set of participating clients, and \mathcal{D} denotes all data of participating clients. For $* \in [\mathcal{I}, \mathcal{T}, \mathcal{F}]$, \mathcal{P}_{*^j} denotes the local prototypes and \mathcal{P}_{*^j} denotes the global prototypes.

3.3. Prototypes as Masks of Missing Modalities

When missing modalities occur, previous work [8] masks missing data with zero tensors. In PmcmFL, prototypes are employed as masks for missing modality representations, thereby incorporating global prior knowledge. Based on this, a task-calibrated training loss and a model-agnostic unimodal inference strategy are proposed.

Task-Calibrated Training Loss. As shown in Figure 2, during local training with complete image-text pairs, the training loss is defined:

$$L_{task} = \mathcal{L}(\mathcal{G}_n(\mathcal{F}_n(h_{nk}^{(i)}, h_{nk}^{(t)})), y_{nk}), \quad (4)$$

where \mathcal{L} denote the task loss function. In the case of local training with text missing, a task-calibrated training loss is constructed using the text prototypes as masks:

$$L_{task} = \mathcal{L}(\mathcal{G}_n(\mathcal{F}_n(h_{nk}^{(i)}, \mathcal{P}_{\mathcal{T}}^j)), y_{nk}), \quad (5)$$

where $\mathcal{P}_{\mathcal{T}}^j$ has the same class as y_{nk} . Similarly, the task-calibrated training loss is defined when images are missing:

$$L_{task} = \mathcal{L}(\mathcal{G}_n(\mathcal{F}_n(\mathcal{P}_{\mathcal{I}}^j, h_{nk}^{(t)})), y_{nk}). \quad (6)$$

With supervision from the task-calibrated loss, the entire model is trained on the original multimodal task, even when there are missing modalities on clients. On the contrary, using zero masks will result in a task-drifted loss. For example, in the case where text is missing, the training loss with zero masks is denoted as $\mathcal{L}(\mathcal{G}_n(\mathcal{F}_n(h_{nk}^{(i)}, \mathbf{0})), y_{nk})$. Essentially, this represents a unimodal training task that depicts

the relationship between the unimodal representation $h_{nk}^{(i)}$ and the ground truth y_{nk} , which leads to inconsistent optimization directions for the model training.

Model-Agnostic Unimodal Inference. During inference with missing modalities, prototypes are employed as masks to assist the global model. Unlike training, where labels are available, we must find corresponding cross-modal prototypes according to embedded representations. To this end, a matching function $m(\cdot)$ is established from hidden representations to prototypes. We use an example to describe the matching process of cross-modal prototypes. Without loss of generality, assume that the model only utilizes images for inference. First, the image i_{nk} is input for computing the image representation $h_{nk}^{(i)}$. Sequentially, the image prototype with the same class $\mathcal{P}_{\mathcal{I}}^j$ is determined using this matching function $\mathcal{P}_{\mathcal{I}}^j = m(h_{nk}^{(i)})$. Following this, the corresponding text prototype $\mathcal{P}_{\mathcal{T}}^j$ is determined according to class j . Finally, the image representation $h_{nk}^{(i)}$ and the text prototype $\mathcal{P}_{\mathcal{T}}^j$ are input into the subsequent modules.

As for matching function $m(\cdot)$, we propose both model-free and model-based matching. Model-free matching involves matching the closest prototype for each representation using a distance metric, such as L1 distance, L2 distance, or cosine similarity. On the other hand, model-based matching involves training tiny models, treating the search of cross-modal prototypes as either a classification or a retrieval task. These tiny models are trained only in the final round of federated communication, incurring negligible overhead to the FL framework. For the classification task, we train a shallow MLP-Classifier using cross-entropy loss. For the retrieval task, inspired by DALLE-2 [28], we sequentially use CLIP loss [27] and MSE loss to train an MLP-Prior to achieve representation transfer and retrieval. We attempt three aggregation strategies for tiny models from different clients: selecting the model with maximum client samples, model aggregation, and model ensemble.

Inspired by MixUp [37], we propose ProtoMix to enrich the semantic information within prototypes used for inference. ProtoMix linearly combines the top- k related prototypes with weights derived from applying the Softmax function to distance metrics, classification probabilities, or retrieval match scores.

Our inference strategy is model-agnostic and can be applied to all multimodal models, as no additional network branches are introduced in training or testing.

3.4. Prototypes as Learned Representation Targets

Due to the non-IID issue, the learned representation distributions in feature space significantly differ among clients (i.e., client drift), leading to an uncoordinated model aggregation. To achieve model aggregation without conflicts, all clients must theoretically have similar local representation

distributions. In PmcmFL, prototypes are used as learned representation targets to guide clients in learning fused representation distributions clustered by class. For this reason, we introduce a proximal term based on the unidirectional CLIP contrastive loss to regularize client training.

Sampling a batch \mathcal{B} from the local dataset, the proximal term can be denoted as:

$$L_{contr} = -\frac{1}{|\mathcal{B}|} \sum_{s=1}^{|\mathcal{B}|} \log \frac{\exp(h_s^\top \cdot \mathcal{P}_s / \tau)}{\sum_{i=1}^{|\mathcal{B}|} \exp(h_s^\top \cdot \mathcal{P}_i / \tau)}, \quad (7)$$

where h_s is the s -th representation in batch, \mathcal{P}_s is its corresponding prototype, and τ is a temperature factor. As the global model gradually converges, the prototypes converge step by step. This proximal term works by pulling representations closer to the prototypes of the same class and pushing representations away from prototypes of different classes so that the learned representations are around the corresponding global prototypes.

Since prototypes are the centroids of class representations, maintaining a certain distance (i.e., fine-grained semantic difference) from each representation, we use CLIP loss to constrain their similarities rather than relying on MSE to constrain their distances. Although the prototype-based proximal term can theoretically be constructed on image representations, text representations, and fused representations separately, we only utilize the last one due to the difficulty in coordinating multiple proximal terms. In this case, the total training loss for each client is the sum of task loss and contrastive loss of fused representations:

$$L = L_{task} + \gamma L_{contr}^f, \quad (8)$$

where γ is the weighting hyper parameter for L_{contr}^f .

4. Experiment

4.1. Experiment Setup

Dataset. Following CreamFL [36], to evaluate the proposed FL framework with a modality-fusion task, we utilize the challenging VQAv2 dataset [9] to approximate a practical FL scenario. For the efficiency of the experiments, we construct a tiny VQA task, one-tenth the scale of the original VQA task. The tiny VQA is a classification task of 310 classes, with 64,000 training samples and 5,000 testing samples. The training data is distributed to 30 clients, employing the Dirichlet distribution ($\alpha = 0.1$) for non-IID data partition [10]. More details are in Appendix C.

Model. For the multiway encoder \mathcal{E} , we utilize the same architecture as BEIT3-base [33] along with its pre-train parameters. For the deep fusion layer \mathcal{F} , the image CLS token and the text CLS token are concatenated and projected through an MLP. For the task head \mathcal{G} , the fusion representation is projected to logits using another MLP.

Methods	Accuracy (%) on 5K Complete Testing Samples					Acc@sum
	10% missing	20% missing	30% missing	40% missing	50% missing	
FedAvg [23] + ignore missing	56.444	53.936	49.990	45.024	38.898	244.292
FedAvg [23] + zero mask	55.360	52.804	49.246	46.378	41.034	244.822
FedAvg [23] + random mask	55.624	52.542	48.164	47.288	41.346	244.964
FedProx [17]	52.506	49.546	46.502	46.862	41.140	236.556
FedIoT [39]	55.010	52.180	47.558	47.582	41.838	244.168
FedPAC [34]	55.028	50.742	46.916	45.930	40.242	238.858
FedHKD [2]	56.286	53.546	50.544	47.832	43.376	251.584
PmmFL(Ours) + FA	56.144	54.366	50.556	48.796	46.168	256.030
PmmFL(Ours) + HKD	56.458	53.926	51.568	49.472	46.394	257.818
PmcmFL (Ours)	56.636*	55.478*	52.256*	49.548*	47.042*	260.960*

Table 1. Comparison of PmcmFL with baselines under various missing rates. * denotes the PmcmFL’s performance is significantly better than existing baselines (paired t-test, $p < 0.05$).

Baseline. We compare our PmcmFL with the previous FL frameworks. Among them, 1) FedAvg [23] and 2) FedProx [17] are widely used methods, 3) FedIoT [39] and 4) CreamFL [36] are methods for multimodal federated learning, 5) FedPAC [34] and 6) FedHKD [2] are state-of-the-art methods based on prototypes. We develop multimodal models on clients across all baseline frameworks to extend them to multimodal FL. We adopt optimal values presented in their respective papers for the hyperparameters in each baseline. To demonstrate the effectiveness of our Prototype Contrast, we further compare PmcmFL with its two variants: 7) PmmFL+FA and 8) PmmFL+HKD, which replace Prototype Contrast with Feature Alignment (FA) [34] and Hyper Knowledge Distillation (HKD) [2], respectively.

To handle missing modalities, we attempt three baseline strategies: 1) ignoring incomplete data, 2) zero masks, 3) Gaussian random masks. The most effective strategy under FedAvg is then applied to other FL frameworks.

Implement Details. To enable fair comparisons, our experiments remain consistent on method-agnostic hyperparameters, including federated communication rounds, local training epochs, client selection rate, learning rate, optimizer parameters, and batch size. For Prototype Contrast, the temperature factor τ is set to 0.07, and the weight γ is searched within [5.0, 1.0, 0.5, 0.1, 0.01] to find the optimal value. Following suggestions from previous work [8], we set an equal missing rate of $q = [0.1, 0.2, 0.3, 0.4, 0.5]$ for each modality. For inference with missing modalities, we set the missing rate of one modality to 100% for intuitive comparison. For top- k ProtoMix, we attempt all possible values for k . More details are in Appendix D.

Evaluation Metric. The metric of VQAv2 is adopted for evaluating our task. We utilize optimal accuracy in the last ten communication rounds as the final performance. Note that all evaluations are conducted with modality-complete testing samples, except in experiments on infer-

ence with missing modalities (Sec. 4.4).

4.2. Main Results

Table 1 displays the accuracy of the global model in all baselines and our PmcmFL. Our PmcmFL framework generally achieves noticeable performance improvement over all baselines in all modality missing rates.

The comparison of three baseline methods for handling missing modalities under FedAvg shows that the Gaussian Random Mask performs best. Compared to ignoring incomplete data, the Mask method significantly improves the performance of federated training with 50% modality missing (a 2.448% boost), which indicates that Mask is effective in handling severe modality missing.

Compared to FedAvg, FedIoT leads to a performance decline (a 0.796% drop on Acc@sum), which indicates that assigning more aggregation weight to multimodal clients no longer works in our task scenarios. Similarly, FedPAC leads to a performance decline (a 6.106% drop on Acc@sum), which is because the feature alignment (FA) employed by FedPAC, a strong regularization that narrows the distance between representations and prototypes through MSE, disrupts the semantic distinctiveness of representations.

Compared to all the baselines, our PmcmFL achieves superior performance (9.376-24.404% boost on Acc@sum), demonstrating the effectiveness of our Prototype Mask and Contrast. Furthermore, as the modality missing rate increases, the performance improvement brought about by our PmcmFL tends to be more significant (a 0.192% boost in 10% missing but a 3.666% boost in 50% missing).

Compared to PmcmFL’s variants, slightly superior performance (3.14-4.93% boost on Acc@sum) indicates that our Prototype Contrast is more generalizable than Feature Alignment and Hyper Knowledge Distillation. We further validate the better performance of PmcmFL compared with CreamFL in scenarios with a 100% missing rate of either

PC	PM	Accuracy (%) on 5K Complete Testing Samples					Acc@sum
		10% missing	20% missing	30% missing	40% missing	50% missing	
		55.624	52.542	48.164	47.288	41.346	244.964
✓		55.948	53.588	50.982	47.422	44.454	252.394
	✓	55.326	54.486	50.858	49.290	45.848	255.808
✓	✓	56.636	55.478	52.256	49.548	47.042	260.960

Table 2. Results of ablation studies under various modality missing rates. PC denotes Prototype Contrast and PM denotes Prototype Mask.

Methods	Accuracy (%) on Unimodal Data			
	Mix-1	Mix-10	Mix-20	Mix-best
Zero Mask	0.996	0.996	0.996	0.996
Random Mask	3.662	3.662	3.662	3.662
L1 Metric	6.358	6.170	6.784	6.784
L2 Metric	5.454	5.238	5.782	6.106
COS Metric	5.524	6.062	6.676	6.938
Classifier(max.)	26.956	27.022	27.022	27.022
Classifier(ens.)	27.090	27.090	27.090	27.090
Classifier(avg.)	27.502	27.092	27.092	27.502
MLP-Prior(max.)	27.052	19.906	8.742	27.052
MLP-Prior(ens.)	27.260	27.280	27.280	27.280
MLP-Prior(avg.)	5.858	5.702	5.996	6.210

Table 3. Inference with 100% text modality missing. Zero Mask and Random Mask are baseline methods for handling inference with missing modalities. Others are our Prototype Mask with various matching algorithms. Our Prototype Mask under Top1 ProtoMix, based on classifier matching with aggregation, achieves the best inference accuracy (27.502%).

modality. The experimental results are in Appendix E.

4.3. Ablation Studies

We study the effect of each PmcmFL component during training. Table 2 displays the results of ablation studies under various modality missing rates.

The results show that Prototype Contrast and Prototype Mask contribute to performance improvement over the baselines, with gains of 7.430% and 11.168% on Acc@sum, respectively. We also found that Prototype Mask provides more significant assistance, primarily contributing to performance improvement in PmcmFL. Moreover, combining Prototype Contrast and Prototype Mask assist local training yields further performance boost.

4.4. Inference with Missing Modalities

Table 3 shows the testing accuracy of the global model in 100% text missing, demonstrating intuitively the performance of PmcmFL in handling inference with missing modalities. We use the global model trained with 30% modality missing, and its accuracy is 52.256% in modality-

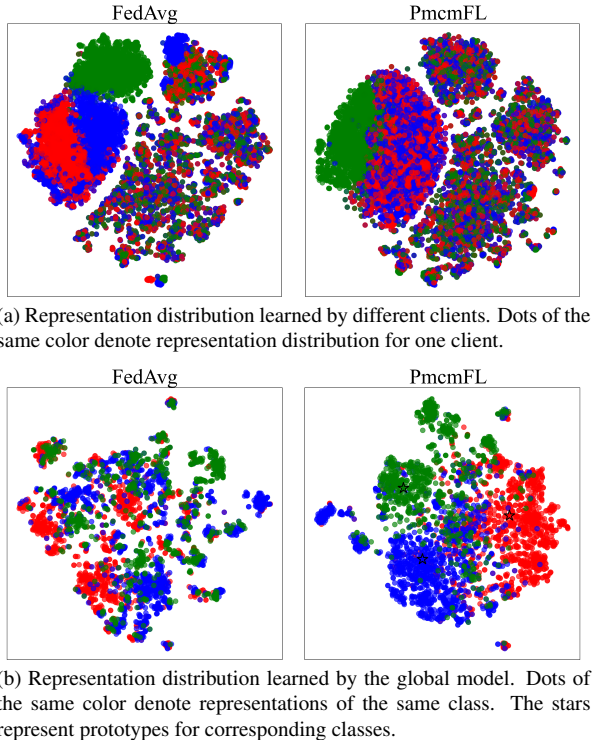


Figure 3. T-SNE visualization for qualitative studies.

complete testing samples. For ProtoMix, top-1, top-10, top-20, and best prototype mix are exhibited.

We can obviously see that the inference accuracy of Zero Mask and Random Mask, serving as baselines, is only 0.996% and 3.662%, respectively, which indicates that the modality missing issues severely impair the model’s inference accuracy. In contrast, Prototype Mask achieves the highest accuracy of 27.502% (a 23.840% boost), demonstrating that our method helps restore modal inference accuracy. Moreover, the experiments also demonstrate the effectiveness of our ProtoMix strategy. More results and discussions can be found in Appendix F.

4.5. Qualitative Studies

We utilize T-SNE [31] for visualization to qualitatively analyze the role of Prototypes Contrast in our FL framework.

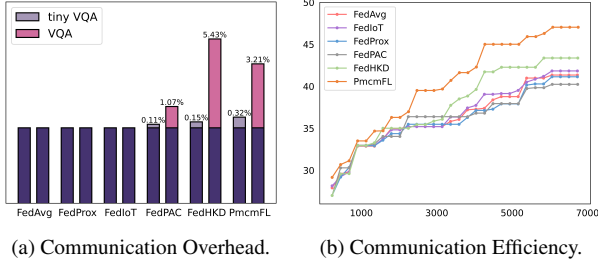


Figure 4. Communication overhead and communication efficiency in six FL frameworks. Figure (a) shows the amount of parameters transmitted by different frameworks in one communication round. Figure (b) shows the optimal performance (%) of the global model when transmitting different parameters (MB).

Figure 3a visualizes fused representation distribution learned by different clients. All testing samples are used in this figure. We can observe that in FedAvg, some dots cluster by clients, indicating that each client forms its individual feature space (client drift). When local models are aggregated into a global model, individual feature spaces hinder the formation of a unified feature space. In contrast, in our PmcmFL, the heterogeneity of feature spaces among various clients (client drift) is reduced due to prototypes acting as representation targets to guide local training.

Figure 3b visualizes the fused representation distribution learned by the global model. We randomly selected samples of three classes in the test set. It can be observed that in FedAvg, dots from different classes are mixed, which is not conducive to subsequent classification tasks. In contrast, in our PmcmFL, dots from different classes cluster around their respective prototypes, which validates our starting point of using prototypes for constructing contrastive loss.

4.6. Overhead and Efficiency of Communication

In our PmcmFL, the parameters transmitted during each federated communication round include model weights and the prototype library.

Figure 4 illustrates different FL frameworks’ communication overhead and communication efficiency. As shown, in our tiny VQA task, PmcmFL introduces only negligible additional communication overhead (+0.32%). In the original VQA task, PmcmFL exhibits even lower communication overhead than FedHKD (+3.21% v.s. +5.43%). Furthermore, we can observe that when transmitting the same amount of parameters, PmcmFL achieves optimal performance, demonstrating that our framework has the highest communication efficiency.

4.7. Robustness to federated hyperparameters

Figure 5 illustrates the performance of various FL Frameworks across different communication rounds, client selection rates, local training epochs, and learning rates. We con-

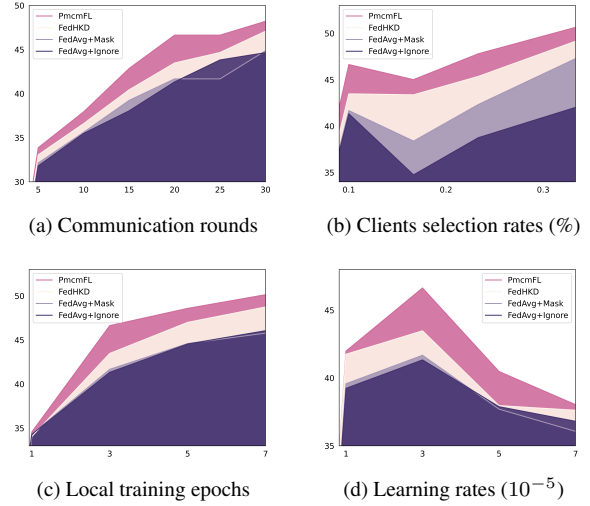


Figure 5. Compare the performance of our PmcmFL with baseline frameworks under different settings of FL hyperparameters. Our PmcmFL consistently achieves the best performance.

duct experiments with 50% modality missing while keeping all hyperparameters constant except the one being investigated. Four representative FL frameworks are compared: 1) FedAvg with ignoring modality-incomplete data, the most common one in practical application; 2) FedAvg with Gaussian Random Mask, the simplest one for handling missing modalities; 3) FedHKD, the existing one with optimal performance; 4) our PmcmFL. The experimental results demonstrate that, under different FL hyperparameters, our PmcmFL consistently achieved optimal performance, showcasing robustness to FL hyperparameters.

5. Conclusion

In this paper, we investigate multimodal federated learning with uncertain modality missing in both training and testing. Our work introduces a prototype library to empower the federated learning framework with the capability to alleviate performance degradation resulting from modality missing. Based on the prototype library, we construct a task-calibrated training loss, a model-agnostic unimodal inference strategy, and a proximal term. The effectiveness of our framework has been validated through comparisons with state-of-the-art methods.

Our forthcoming efforts will center on constructing a prototype library with richer semantics and extending Prototype Mask to a data augmentation method. Alternatively, we plan to improve the prototype matching to achieve better performance in inference with missing modalities. Furthermore, we recognize the potential of employing prototypes to address challenges related to missing or inaccurate labels, and we also intend to explore this avenue.

References

- [1] Hangbo Bao, Li Dong, Songhao Piao, and Furu Wei. BEiT: BERT pre-training of image transformers. In *ICLR*, 2022. [2](#), [4](#)
- [2] Huancheng Chen, Chaining Wang, and Haris Vikalo. The best of both worlds: Accurate global and personalized models through federated learning with data-free hyperknowledge distillation. In *ICLR*, 2023. [2](#), [3](#), [6](#)
- [3] Jiayi Chen and Aidong Zhang. Fedmsplit: Correlation-adaptive federated multi-task learning across multimodal split networks. In *Proceedings of the 28th ACM SIGKDD Conference on Knowledge Discovery and Data Mining*, pages 87–96, 2022. [1](#), [3](#)
- [4] Xi Chen, Xiao Wang, Soravit Changpinyo, A. J. Piergiovanni, Piotr Padlewski, Daniel Salz, Sebastian Goodman, Adam Grycner, Basil Mustafa, Lucas Beyer, Alexander Kolesnikov, Joan Puigcerver, Nan Ding, Keran Rong, Hassan Akbari, Gaurav Mishra, Linting Xue, Ashish V. Thapliyal, James Bradbury, and Weicheng Kuo. Pali: A jointly-scaled multilingual language-image model. In *ICLR*, 2023. [1](#)
- [5] Yutong Dai, Zeyuan Chen, Junnan Li, Shelby Heinecke, Lichao Sun, and Ran Xu. Tackling data heterogeneity in federated learning with class prototypes. In *AAAI*, pages 7314–7322, 2023. [2](#), [3](#)
- [6] Jacob Devlin, Ming-Wei Chang, Kenton Lee, and Kristina Toutanova. BERT: pre-training of deep bidirectional transformers for language understanding. pages 4171–4186, 2019. [4](#)
- [7] Alexey Dosovitskiy, Lucas Beyer, Alexander Kolesnikov, Dirk Weissenborn, Xiaohua Zhai, Thomas Unterthiner, Mostafa Dehghani, Matthias Minderer, Georg Heigold, Sylvain Gelly, Jakob Uszkoreit, and Neil Houlsby. An image is worth 16x16 words: Transformers for image recognition at scale. In *ICLR*, 2021. [4](#)
- [8] Tiantian Feng, Digbalay Bose, Tuo Zhang, Rajat Hebbar, Anil Ramakrishna, Rahul Gupta, Mi Zhang, Salman Avestimehr, and Shrikanth Narayanan. Fedmultimodal: A benchmark for multimodal federated learning. In *Proceedings of the 29th ACM SIGKDD Conference on Knowledge Discovery and Data Mining*, pages 4035–4045, 2023. [1](#), [2](#), [3](#), [4](#), [6](#)
- [9] Yash Goyal, Tejas Khot, Douglas Summers-Stay, Dhruv Batra, and Devi Parikh. Making the V in VQA matter: Evaluating the role of image understanding in visual question answering. In *CVPR*, pages 6325–6334, 2017. [5](#)
- [10] Tzu-Ming Harry Hsu, Hang Qi, and Matthew Brown. Measuring the effects of non-identical data distribution for federated visual classification. *CoRR*, abs/1909.06335, 2019. [5](#)
- [11] Wenke Huang, Mang Ye, and Bo Du. Learn from others and be yourself in heterogeneous federated learning. In *CVPR*, pages 10133–10143, 2022. [1](#)
- [12] Wenke Huang, Mang Ye, Zekun Shi, He Li, and Bo Du. Rethinking federated learning with domain shift: A prototype view. In *CVPR*, pages 16312–16322, 2023. [2](#), [3](#)
- [13] Wonjae Kim, Bokyung Son, and Ildoo Kim. Vilt: Vision-and-language transformer without convolution or region supervision. In *Proceedings of the 38th International Conference on Machine Learning*, pages 5583–5594, 2021. [2](#)
- [14] Huy Q Le, Minh NH Nguyen, Chu Myaet Thwal, Yu Qiao, Chaoning Zhang, and Choong Seon Hong. Fedmekt: Distillation-based embedding knowledge transfer for multimodal federated learning. *arXiv preprint arXiv:2307.13214*, 2023. [1](#)
- [15] Jingzhi Li, Fengling Li, Lei Zhu, Hui Cui, and Jingjing Li. Prototype-guided knowledge transfer for federated unsupervised cross-modal hashing. In *ACM MM*, pages 1013–1022, 2023. [3](#)
- [16] Qinbin Li, Bingsheng He, and Dawn Song. Model-contrastive federated learning. In *CVPR*, pages 10713–10722, 2021. [1](#)
- [17] Tian Li, Anit Kumar Sahu, Manzil Zaheer, Maziar Sanjabi, Ameet Talwalkar, and Virginia Smith. Federated optimization in heterogeneous networks. In *Proceedings of Machine Learning and Systems*, 2020. [1](#), [6](#)
- [18] Xinting Liao, Weiming Liu, Chaochao Chen, Pengyang Zhou, Huabin Zhu, Yanchao Tan, Jun Wang, and Yue Qi. Hyperfed: Hyperbolic prototypes exploration with consistent aggregation for non-iid data in federated learning. In *IJCAI*, pages 3957–3965, 2023. [2](#), [3](#)
- [19] Jiale Liu, Yu-Wei Zhan, Xin Luo, Zhen-Duo Chen, Yongxin Wang, and Xin-Shun Xu. Prototype-based layered federated cross-modal hashing. In *ICASSP*, pages 1–2, 2023.
- [20] Feng Lyu, Cheng Tang, Yongheng Deng, Tong Liu, Yongmin Zhang, and Yaoyue Zhang. A prototype-based knowledge distillation framework for heterogeneous federated learning. In *43rd IEEE International Conference on Distributed Computing Systems*, pages 1–11, 2023. [2](#), [3](#)
- [21] Mengmeng Ma, Jian Ren, Long Zhao, Sergey Tulyakov, Cathy Wu, and Xi Peng. SMIL: multimodal learning with severely missing modality. In *AAAI*, pages 2302–2310, 2021. [2](#)
- [22] Mengmeng Ma, Jian Ren, Long Zhao, Davide Testuggine, and Xi Peng. Are multimodal transformers robust to missing modality? In *CVPR*, pages 18156–18165, 2022. [2](#)
- [23] Brendan McMahan, Eider Moore, Daniel Ramage, Seth Hampson, and Blaise Agüera y Arcas. Communication-efficient learning of deep networks from decentralized data. In *Proceedings of the 20th International Conference on Artificial Intelligence and Statistics*, pages 1273–1282, 2017. [1](#), [6](#)
- [24] Matías Mendieta, Taojiannan Yang, Pu Wang, Minwoo Lee, Zhengming Ding, and Chen Chen. Local learning matters: Rethinking data heterogeneity in federated learning. In *CVPR*, pages 8387–8396, 2022. [1](#)
- [25] Zhiliang Peng, Li Dong, Hangbo Bao, Qixiang Ye, and Furu Wei. BEiT v2: Masked image modeling with vector-quantized visual tokenizers. 2022. [2](#), [4](#)
- [26] Liangqiong Qu, Yuyin Zhou, Paul Pu Liang, Yingda Xia, Feifei Wang, Ehsan Adeli, Li Fei-Fei, and Daniel L. Rubin. Rethinking architecture design for tackling data heterogeneity in federated learning. In *CVPR*, pages 10051–10061, 2022. [1](#)
- [27] Alec Radford, Jong Wook Kim, Chris Hallacy, Aditya Ramesh, Gabriel Goh, Sandhini Agarwal, Girish Sastry,

- Amanda Askell, Pamela Mishkin, Jack Clark, et al. Learning transferable visual models from natural language supervision. In *Proceedings of the 38th International Conference on Machine Learning*, pages 8748–8763, 2021. [2](#), [5](#)
- [28] Aditya Ramesh, Prafulla Dhariwal, Alex Nichol, Casey Chu, and Mark Chen. Hierarchical text-conditional image generation with CLIP latents. *CoRR*, abs/2204.06125, 2022. [5](#)
- [29] Jake Snell, Kevin Swersky, and Richard S. Zemel. Prototypical networks for few-shot learning. In *NeurIPS*, pages 4077–4087, 2017. [3](#)
- [30] Yue Tan, Guodong Long, Lu Liu, Tianyi Zhou, Qinghua Lu, Jing Jiang, and Chengqi Zhang. Fedproto: Federated prototype learning across heterogeneous clients. In *AAAI*, pages 8432–8440, 2022. [3](#)
- [31] Laurens Van der Maaten and Geoffrey Hinton. Visualizing data using t-sne. *Journal of machine learning research*, 9 (11), 2008. [7](#)
- [32] Hu Wang, Yuanhong Chen, Congbo Ma, Jodie Avery, Louise Hull, and Gustavo Carneiro. Multi-modal learning with missing modality via shared-specific feature modelling. In *CVPR*, pages 15878–15887, 2023. [3](#)
- [33] Wenhui Wang, Hangbo Bao, Li Dong, Johan Bjorck, Zhiliang Peng, Qiang Liu, Kriti Aggarwal, Owais Khan Mohammed, Saksham Singhal, Subhojit Som, and Furu Wei. Image as a foreign language: BEIT pretraining for vision and vision-language tasks. In *CVPR*, pages 19175–19186, 2023. [1](#), [2](#), [4](#), [5](#)
- [34] Jian Xu, Xinyi Tong, and Shao-Lun Huang. Personalized federated learning with feature alignment and classifier collaboration. In *ICLR*, 2023. [2](#), [3](#), [6](#)
- [35] Jiahui Yu, Zirui Wang, Vijay Vasudevan, Legg Yeung, Mojtaba Seyedhosseini, and Yonghui Wu. Coca: Contrastive captioners are image-text foundation models. *Transactions on Machine Learning Research*, 2022. [1](#)
- [36] Qiyang Yu, Yang Liu, Yimu Wang, Ke Xu, and Jingjing Liu. Multimodal federated learning via contrastive representation ensemble. In *ICLR*, 2023. [1](#), [2](#), [3](#), [5](#), [6](#)
- [37] Hongyi Zhang, Moustapha Cissé, Yann N. Dauphin, and David Lopez-Paz. mixup: Beyond empirical risk minimization. In *ICLR*, 2018. [5](#)
- [38] Jinming Zhao, Ruichen Li, and Qin Jin. Missing modality imagination network for emotion recognition with uncertain missing modalities. In *Proceedings of the 59th Annual Meeting of the Association for Computational Linguistics and the 11th International Joint Conference on Natural Language Processing*, pages 2608–2618, 2021. [2](#)
- [39] Yuchen Zhao, Payam M. Barnaghi, and Hamed Haddadi. Multimodal federated learning on iot data. In *Seventh IEEE/ACM International Conference on Internet-of-Things Design and Implementation*, pages 43–54, 2022. [1](#), [2](#), [3](#), [6](#)
- [40] Zhuangdi Zhu, Junyuan Hong, and Jiayu Zhou. Data-free knowledge distillation for heterogeneous federated learning. In *Proceedings of the 38th International Conference on Machine Learning*, pages 12878–12889, 2021. [1](#)

Multimodal Federated Learning with Missing Modality via Prototype Mask and Contrast

Supplementary Material

A. Algorithm

Algorithm 2 and Algorithm 1 illustrate the flowcharts of our PmcmFL during training and inference, respectively.

Algorithm 1: Inference of PmcmFL.

Input: Server model $(\mathcal{E}, \mathcal{F}, \mathcal{G})$, Testing set.
Output: Labels for classification tasks

- 1 **if** input is an image-text pair (i, t) **then**
- 2 Compute $logits = \mathcal{G}(\mathcal{F}(\mathcal{E}(i, t)))$
- 3 **end**
- 4 **else if** input is an image i **then**
- 5 Compute the image representation $h^{(i)} = \mathcal{E}(i)$;
- 6 Search for the corresponding image prototype $\mathcal{P}_{\mathcal{I}}^j$ using matching function $m(h^{(i)})$;
- 7 Find the corresponding text prototype $\mathcal{P}_{\mathcal{T}}^j$ through the association in the prototype library;
- 8 Compute $logits = \mathcal{G}(\mathcal{F}(h^{(i)}, \mathcal{P}_{\mathcal{T}}^j))$;
- 9 **end**
- 10 **else if** input is text t **then**
- 11 Compute the text representation $h^{(t)} = \mathcal{E}(t)$;
- 12 Search for the corresponding text prototype $\mathcal{P}_{\mathcal{T}}^j$ using matching function $m(h^{(t)})$;
- 13 Find the corresponding text prototype $\mathcal{P}_{\mathcal{I}}^j$ through the association in the prototype library;
- 14 Compute $logits = \mathcal{G}(\mathcal{F}(\mathcal{P}_{\mathcal{I}}^j, h^{(t)}))$;
- 15 **end**
- 16 Calculate probability distribution and predict the label: $\hat{y} = \text{argmax Softmax}(logits)$

B. Discussion on Model Architecture

B.1. Different Encoding Modes

Owing to modality-specific expert networks and shared self-attention layers, Multiway Transformer can switch between different encoding modes. **In this section, we introduce the different encoding modes in detail.**

The input images and text are initially processed into sequences of tokens involving patchify/tokenization and positional encoding. The initial token sequences (the image token sequence, the text token sequence, and the image-text token sequence) can be represented as:

$$z_i^0 = [z_{i0}, z_{i1}, \dots, z_{iN_i}], \quad (9)$$

$$z_t^0 = [z_{t0}, z_{t1}, \dots, z_{tN_t}], \quad (10)$$

$$z^0 = \text{cat}(z_i^0, z_t^0) = [z_{i0}, \dots, z_{iN_i}, z_{t0}, \dots, z_{tN_t}], \quad (11)$$

where z_{i*} denotes the image token, z_{t*} denotes the text token, z_{i0} denotes the image CLS token, z_{t0} denotes the text CLS token, N_i and N_t denote the number of image tokens and text tokens respectively.

For the Shared Multi-Head Self-Attention module at l -th encoding layer, we represent it as $Attention^l(\cdot)$. For the Modality-Specific Expert Networks at l -th encoding layer, we use $FFN_i^l(\cdot)$ and $FFN_t^l(\cdot)$ to respectively represent the vision expert network and the language expert network. For the sake of clarity, we have omitted residual connections and layer normalization.

When dealing with only image inputs, Multiway Transformer utilizes the attention module and the visual expert network at each layer:

$$z_i^l = FFN_i^l(Attention^l(z_i^{l-1})). \quad (12)$$

When dealing with only text inputs, Multiway Transformer utilizes the attention module and the language expert network at each layer:

$$z_t^l = FFN_t^l(Attention^l(z_t^{l-1})). \quad (13)$$

When dealing with image-text pairs, Multiway Transformer first employs the shared self-attention module for cross-modal interaction:

$$a^l = \text{cat}(a_i^l, a_t^l) = Attention^l(z^{l-1}). \quad (14)$$

Subsequently, individual expert networks are applied to tokens from the corresponding modality:

$$z^l = \text{cat}(FFN_i^l(a_i^l), FFN_t^l(a_t^l)). \quad (15)$$

B.2. Decoupling Framework and Model

It is important to highlight that **the encoders used in our PmcmFL are not limited to the Multiway Transformer encoder.** In fact, our framework is flexible to incorporate with vision/language encoders of other architectures.

Figure 6 illustrates the general architecture of multimodal models and the architecture we use. Just like our current architecture, general multimodal models consist of three main parts: encoders, a fusion layer, and a task head. They can be easily transplanted into our PmcmFL. To elaborate, we can effortlessly compute prototypes by utilizing the outputs of the visual encoder, language encoder, and fusion module. If the fusion module employs the Transformer

Algorithm 2: Training of PmcmFL.

Input: Number of federated communication rounds T , number of clients C , number of local epochs E , server model, local model $(\mathcal{E}_n, \mathcal{F}_n, \mathcal{G}_n)$, local learning rate η , dataset $\mathcal{D}_n = (\mathcal{M}_n, \mathcal{I}_n, \mathcal{T}_n)$ of the n -th client and fraction of clients s that are selected to perform computation in each round.

Output: The final server model’s parameters ω^T

```
1 ServerExecutes:
2   Initialize  $\omega^0$  randomly;
3   Initialize global prototypes  $\mathcal{P}_{\mathcal{I}-local}, \mathcal{P}_{\mathcal{T}-local}, \mathcal{P}_{\mathcal{F}-local}$  with zero tensors;
4   for  $t = 1, 2, \dots, T$  do
5     Compute global prototypes  $\mathcal{P}_{\mathcal{I}}, \mathcal{P}_{\mathcal{T}}, \mathcal{P}_{\mathcal{F}}$  according to Equation 1 2 3;
6      $\mathcal{P}_{\mathcal{I}-local}, \mathcal{P}_{\mathcal{T}-local}, \mathcal{P}_{\mathcal{F}-local} \leftarrow [], [], []$ ;
7      $S_t \leftarrow$  random set of  $\max(s \cdot C, 1)$  clients;
8     for each client  $n$  in  $S_t$  do
9       send the global model’s parameters  $\omega^{t-1}$  and global prototypes  $\mathcal{P}_{\mathcal{I}}, \mathcal{P}_{\mathcal{T}}, \mathcal{P}_{\mathcal{F}}$  to client  $n$ ;
10       $\omega_n^t, \mathcal{P}_{\mathcal{I}n}, \mathcal{P}_{\mathcal{T}n}, \mathcal{P}_{\mathcal{F}n} \leftarrow$  ClientLocalTraining ( $n, t, \omega^{t-1}, \mathcal{P}_{\mathcal{I}}, \mathcal{P}_{\mathcal{T}}, \mathcal{P}_{\mathcal{F}}$ );
11       $\mathcal{P}_{\mathcal{I}-local}, \mathcal{P}_{\mathcal{T}-local}, \mathcal{P}_{\mathcal{F}-local} \leftarrow \mathcal{P}_{\mathcal{I}-local} + \mathcal{P}_{\mathcal{I}n}, \mathcal{P}_{\mathcal{T}-local} + \mathcal{P}_{\mathcal{T}n}, \mathcal{P}_{\mathcal{F}-local} + \mathcal{P}_{\mathcal{F}n}$ ;
12    end
13    Local models are aggregated into the global model:  $\omega^t = \sum_{n \in S_t} \frac{|\mathcal{D}_n|}{|\mathcal{D}|} \omega_n^t$ 
14  end
15 ClientLocalTraining ( $n, t, \omega^{t-1}, \mathcal{P}_{\mathcal{I}}, \mathcal{P}_{\mathcal{T}}, \mathcal{P}_{\mathcal{F}}$ ):
16  for epoch  $i = 1, 2, \dots, E$  do
17    Local update  $\omega_n^{(t,i)} \leftarrow \omega_n^{(t,i-1)} - \eta \nabla L(\mathcal{D}_n, \mathcal{P}_{\mathcal{I}}, \mathcal{P}_{\mathcal{T}}, \mathcal{P}_{\mathcal{F}}; \omega_n^{(t-1,i-1)})$  according to Equation 8 ;
18  end
19  Compute local prototypes  $\mathcal{P}_{\mathcal{I}n}, \mathcal{P}_{\mathcal{T}n}, \mathcal{P}_{\mathcal{F}n}$  according to Equation 1 2 3;
20  Return  $\omega_n^t, \mathcal{P}_{\mathcal{I}n}, \mathcal{P}_{\mathcal{T}n}, \mathcal{P}_{\mathcal{F}n}$ ;
```

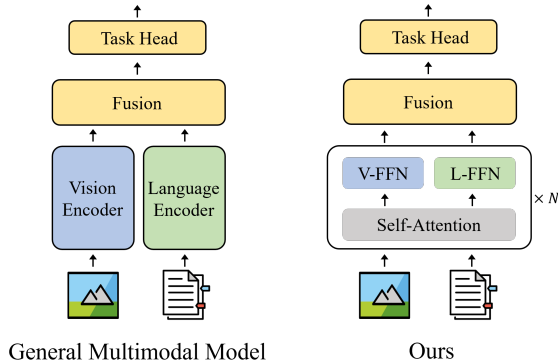


Figure 6. Comparison of general multimodal models and the multimodal model we used. The main difference lies in the architecture of the encoder: we adopt a multi-path encoder, whereas general multimodal models use modality-specific encoders.

architecture, it could be a wise move to integrate a bottleneck module after the modality-specific encoders to reduce communication overhead.

Our architecture differs from the general one in its superior ability in handling multimodal interaction. In our setup, the multiway encoder not only functions as usual but also doubles as a dual-stream fusion module when data from

both modalities is in play.

C. Datasets

C.1. Tiny VQA

Our tiny VQA is a scaled-down version, reducing both label quantity and training data volume to one-tenth of the original VQA task. The original VQA is commonly seen as a classification task with over 3,000 classes, supported by a vast training dataset exceeding 640,000 samples. We refine the labels by excluding those with fewer than 180 occurrences, reshaping VQA into a classification challenge with 310 classes. For training, we randomly chose 64,000 image-text pairs, equivalent to one-tenth of the combined original VQA task training and validation sets. Additionally, our test set comprises 5,000 random image-text pairs randomly selected, ensuring none overlap with the training set. All experiments were conducted on tiny VQA, except when compared with CreamFL.

C.2. Visualization for Data Distribution

To simulate real-world scenarios, we distributed the training data of tiny VQA across 30 clients, using a Dirichlet distribution with a hyperparameter of 0.1 as the basis for non-

IID partitioning. Additionally, to simulate uncertain modality loss, we assigned a fixed missing rate for each modality on every client, thereby conforming to the Bernoulli distribution. In our experiments, we considered five missing ratios: 10%, 20%, 30%, 40%, and 50%. We visualized the data/modality distribution to illustrate the corresponding non-IIDness and modalities missingness as follows.

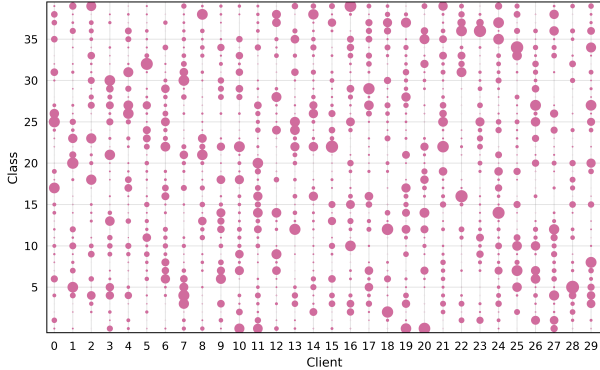


Figure 7. The data distribution of diverse classes on each client. The size of the dots represents the amount of data.

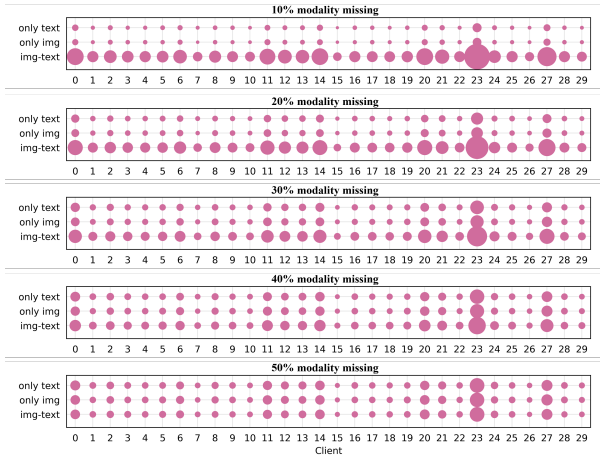


Figure 8. The modality distribution of various clients under different modality missing rates. The size of the dots represents the amount of data.

Visualization for Non-IIDness. We randomly selected 40 classes from a pool of 310, visualizing their distribution across various clients. Figure 7 displays the diversified results of the visualization, indicating the heterogeneous class distribution across clients.

Visualization for Modality Missingness. We visualized the modality distribution on various clients under different modality missing rates. Figure 8 displays the visualization results, showing the diversified modality distribution.

D. Implementation Details

We will go through the implementation details of each experiment one by one.

Main Experiments. The main experiment establishes consistent missing rates for each modality, specifically 0.1, 0.2, 0.3, 0.4, and 0.5. For federal learning hyperparameters, we set the communication rounds to 30. In each round, 5 clients are selected to participate in training (client selection rate is 0.167). The local iteration epochs are set to 3, and the learning rate is fixed at $3e-5$. For the optimizer, we use the AdamW optimizer with a weight decay set to $1e-4$, a momentum of 0.9, and β of [0.9, 0.98]. All experiments are conducted on 4 NVIDIA RTX 4090 GPUs using distributed data parallelism, with a total batch size of 48 (12 per GPU). For the training loss, we set the temperature factor to 0.07, and the hyperparameter search for prototype contrast loss weights is performed over [5.0, 1.0, 0.5, 0.1, 0.01].

Ablation Studies. The hyperparameter settings for the ablation experiments are the same as those for the main experiment.

Inference with Missing Modalities. We employed the top-performing model, trained with a 30% modality missing in our main experiments, for inference. We deliberately omitted 100% of the text modality during this inference, focusing solely on uni-modal inference for images.

For model-based matching, we trained tiny models on each client in the final round of federated communication. The classification-based matching utilizes a 2.2M MLP architecture, accounting for less than 1% of the communication round’s overhead. The model takes image representations as input for a 310-class classification task and undergoes 100 epochs of training on each client, with a single GPU training time of under 1 minute.

Similarly, the retrieval-based matching employs a 2.9M MLP architecture, constituting approximately 1% of the communication round’s overhead. This model takes image representations as input and generates corresponding image prototypes. Its training involves an initial 200 epochs with contrastive loss, followed by 500 epochs of MSE loss. The training time on a single GPU is approximately 3-5 minutes.

We experimented with three strategies to explore the utilization of small models from various clients: selecting the model with the maximum client samples, model parameter aggregation through FedAvg, and model ensemble. The first strategy entails choosing the model from the client with the most data samples among the 30 clients. The model aggregation strategy combines the 30 small models through FedAvg. The model ensemble method merges classification probabilities or retrieval scores from individual models through weighted aggregation, with weights determined by the sample quantities of the respective clients.

Qualitative Studies. We chose the optimal model trained in the main experiment with 50% modality miss-

ing for quantitative experiments. The client models used are those employed in aggregating the best global model.

Communication Efficiency. The experiments on communication efficiency utilized the results derived from the main experiment.

Verification of Robustness. We tested PmcmFL’s robustness for varying communication rounds, client selection rates, local training epochs, and learning rates. The initial experiment had a baseline of 20 communication rounds, selecting 3 clients per round, with local epochs at 3 and a learning rate of $3e-5$. All other hyperparameter settings matched the main experiment. Federated communication rounds are chosen from [5, 10, 15, 20, 25, 30], the number of selected clients is chosen from [3, 5, 7, 10], local iteration epochs are chosen from [1, 3, 5, 7], and the learning rate is chosen from [$1e-5$, $3e-5$, $5e-5$, $7e-5$].

E. Comparison in Specific Task Scenarios

Similar to CreamFL, we conducted experiments in specific scenarios where there are only unimodal clients and modality-complete multimodal clients. We train models on over 3000 of the most frequent answers (the original VQA task) and report the inference accuracy on 5K testing samples. Table 4 shows the results.

Methods	Accuracy
FedAvg	52.54
FedIoT	53.06
FedMD	57.43
FedET	59.90
FedGEMS	60.23
reamFL+Avg	58.64
reamFL+IoT	59.64
CreamFL	62.12
PmcmFL(Ours)	65.53

Table 4. Comparison of PmcmFL with baselines in specific task scenarios.

The results show our framework also achieves SOTA performance (a 3.38% boost compared with CreamFL). This suggests that PmcmFL is equally applicable to specific task scenarios considered by previous works and outperforms methods specifically designed for such scenarios.

We believe that this performance improvement mainly stems from the utilization of the Multiway Transformer encoder, which excels in modality fusion and thus benefits the task. This reflects the advantage of our federated framework compared with CreamFL, which cannot train the modality fusion module on the client.

F. Additional Discussion of Unimodal Inference

F.1. Accuracy of Various Matching Strategies

Table 5 displays the matching accuracy of each matching strategy on 5K testing data.

Methods	Matching Accuracy (%)			
	Top1	Top5	Top10	Top20
L1 Metric	2.46	5.94	10.78	28.46
L2 Metric	1.04	3.14	4.94	11.86
COS Metric	1.04	3.32	6.84	27.04
Classifier(max)	19.10	46.28	50.80	55.16
Classifier(ens)	22.34	54.38	62.72	69.14
Classifier(avg)	23.20	51.16	57.18	62.74
MLP-Piror(max)	19.56	41.92	42.62	43.46
MLP-Piror(ens)	21.70	47.92	52.38	56.16
MLP-Piror(avg)	0.36	4.32	5.36	9.72

Table 5. The matching accuracy of various matching strategies under top-1, top-5, top-10, and top-20 matches.

We can see that there is a significant difference in the matching accuracy of prototype matching strategies with different approaches. The top-1 matching accuracy of the model-free matching strategy is only around 1.04-2.46%, while the top-1 prototype matching accuracy of the model-based matching strategy is approximately 19.10-23.20% (except for MLP-Prior with parameter aggregation).

In addition, compared to the top-1 matching accuracy, the matching accuracy for top-k ($k=5, 10, 20$) shows significant improvement. This suggests that considering more prototypes may lead to obtaining more closely matched prototypes, which forms the basis for our proposal of ProtoMix.

Compared to Table 3 in the main text, we observe a positive correlation between top-1 prototype matching accuracy and accuracy of inference with missing modalities. The positive correlation is reasonable and the effect we desire, which also indicates that, for higher accuracy of inference with missing modalities, we should strive to improve the accuracy of prototype matching. In fact, when we perform unimodal inference using the corresponding prototypes (prototype matching accuracy is 100%), its accuracy can reach 43.314%, which is only 8.942% lower than the modality-complete inference.

F.2. Additional Analysis of ProtoMix

Figure 9 displays all possible ProtoMix results for nine baseline matching strategies.

We observe that almost all matching strategies benefit from ProtoMix, indicating that our proposed strategy of augmenting prototype semantics is effective. However, the

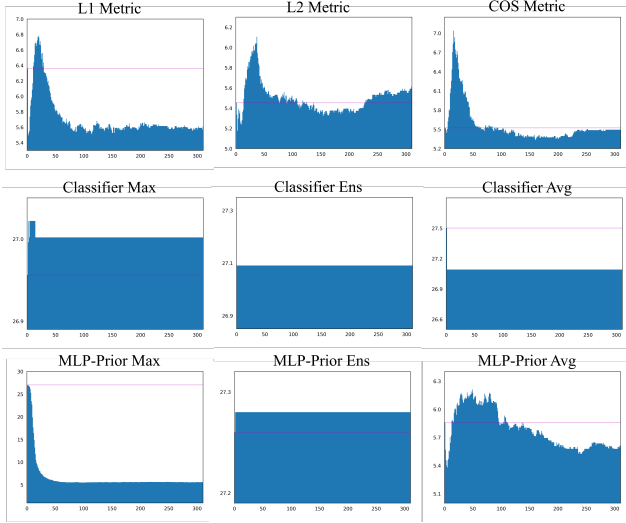


Figure 9. All possible ProtoMix results for nine matching strategies. The horizontal axis represents the k values in the top- k ProtoMix, while the vertical axis represents the corresponding accuracy of inference with missing modalities. The horizontal line represents the accuracy of the top-1 ProtoMix.

performance improvement brought by Top- k ProtoMix is very limited and does not correspond to the accuracy of Top- k prototype matching, which suggests that there is still significant space for improvement in our ProtoMix.

Additionally, we observed significant differences in the performance of ProtoMix under different matching strategies, and we will analyze them one by one. There are two key factors influencing the performance of ProtoMix: prototype matching accuracy and matching confidence.

For the three model-free matching strategies, both matching accuracy and confidence are relatively low. The results indicate that combining top- k prototypes with confidence-weighted fusion results in prototypes with more accurate semantics.

For the three classifier-based matching strategies, their matching accuracy is generally moderate, but the confidence in the top-1 match is exceptionally high. We observed that both a single classifier and a parameter-aggregated classifier have 19.10% matching accuracy but almost boast over 99% confidence in the top-1 class. The results in very little semantic information from other prototypes were obtained when combining top- k prototypes with confidence-weighted fusion. Consequently, the inference accuracy remains the same regardless of how many prototypes are fused. This limitation stems from the poor generalization ability of the classifier, as it tends to overfit the uneven distribution of client data during training on the client side.

For the three retrieval-based matching strategies, we observed that a single prior has 19.56% prototype matching

accuracy and possesses a top-1 retrieval score with less prominent confidence, creating a difference between the maximum prior and the ensemble prior. However, since parameter aggregation does not apply to non-classification tasks, the aggregated model exhibits low matching accuracy and confidence, leading to performance comparable to model-free matching strategies.

G. Additional Visualization

G.1. Representation Distribution among Clients

We visualized more representation distributions learned by various clients. Figure 10 displays the visualized results. We observe that, compared to the baseline method FedAvg, our PmcmFL reduces the heterogeneity in the feature space among clients (i.e., mitigates client drift).

G.2. Representation Distribution among Classes

We visualized more representation distributions learned by the global model among various classes. Figure 11 displays the visualized results. We can observe that, compared to the baseline method, our PmcmFL has the ability to cluster representations by class.

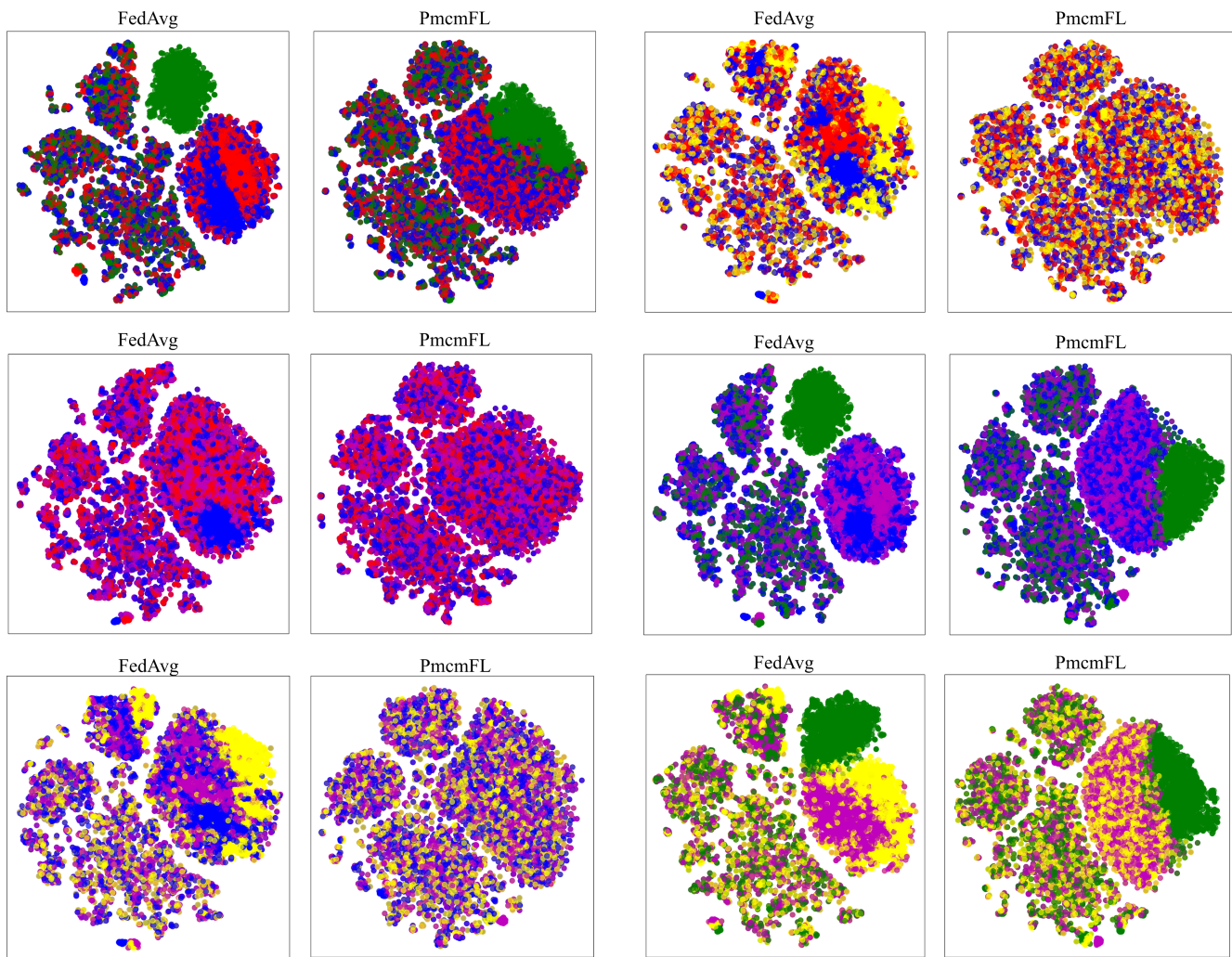


Figure 10. Representation Distribution among Clients. Dots of the same color come from the same client. Compared to the baseline, our PmcFL reduces heterogeneity between clients.

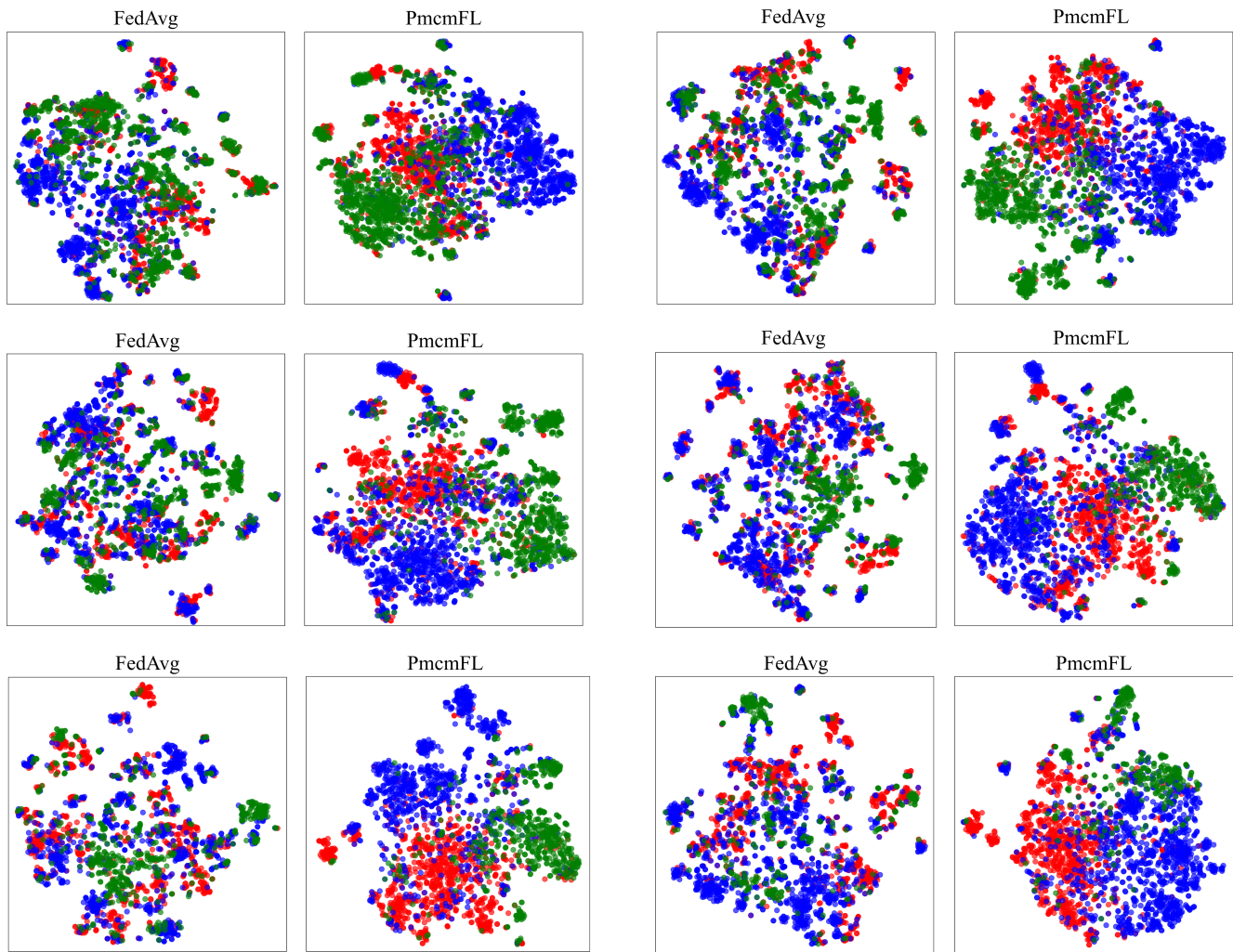


Figure 11. Representation Distribution among Classes. Dots of the same color represent the fused representation of the same class. Compared to the baseline, our PmcFL can cluster representations by class.